EMBO reports

scientific report

Hexameric ring structure of human MCM10 DNA replication factor

Andrei L. Okorokov[1,2+], Alastair Waugh[2], Julie Hodgkinson[3], Andal Murthy[2], Hye Kyung Hong[1,2], Elisabetta Leo[2], Michael B. Sherman[4], Kai Stoeber[1,2], Elena V. Orlova[3++] & Gareth H. Williams[1,2]

[1]Department of Pathology, University College London, London, UK, [2]Wolfson Institute for Biomedical Research, University College London, London, UK, [3]School of Crystallography, Birkbeck College, London, UK, and [4]Department of Biochemistry & Molecular Biology, University of Texas Medical Branch, Galveston, Texas, USA

The DNA replication factor minichromosome maintenance 10 (MCM10) is a conserved, abundant nuclear protein crucial for origin firing. During the transition from pre-replicative complexes to pre-initiation complexes, MCM10 recruitment to replication origins is required to provide a physical link between the MCM2–7 complex DNA helicase and DNA polymerases. Here, we report the molecular structure of human MCM10 as determined by electron microscopy and single-particle analysis. The MCM10 molecule is a ring-shaped hexamer with large central and smaller lateral channels and a system of inner chambers. This structure, together with biochemical data, suggests that this important protein uses its architecture to provide a docking module for assembly of the molecular machinery required for eukaryotic DNA replication.

Keywords: DNA replication; MCM10; DNA binding; electron microscopy; structure

EMBO reports (2007) **8**, 925–930. doi:10.1038/sj.embor.7401064

INTRODUCTION

Eukaryotic cells initiate DNA replication from multiple replication origins scattered along each chromosome. The activation of replication origins is a two-step mechanism that begins with the ordered formation of a macromolecular protein complex, called the pre-replicative complex (pre-RC), during late mitosis and early G1 phase (Bell & Dutta, 2002; Mendez & Stillman, 2003). The second step is dependent on cyclin-dependent kinases and the Dbf4^{ASK}-dependent Cdc7 kinase, which promote the transition from pre-RCs to pre-initiation complexes (pre-ICs) throughout S phase. This step involves the recruitment of minichromosome maintenance 10 (Mcm10), Cdc45 and additional initiator proteins to the origin, which collectively are able to promote unwinding of the origin and to recruit DNA polymerases (Bell & Dutta, 2002; Mendez & Stillman, 2003; Takeda & Dutta, 2005).

Understanding the role of the Mcm10 protein in this process and in supporting the structure and function of eukaryotic replication forks is still limited. *Mcm10* was originally isolated in the screen for *Saccharomyces cerevisiae* mutants that had defects in maintaining minichromosomes, but shares no sequence homology with the Mcm2–7 conserved family (Maine *et al*, 1984; Merchant *et al*, 1997; Maiorano *et al*, 2006).

Studies in yeast have shown that the binding of Mcm10 to chromatin is independent of chromatin-bound Mcm2–7 proteins, but requires interaction with the chromatin-bound origin recognition complex, whereas in *Xenopus* and human cells, Mcm2–7 complex loading is required for Mcm10 recruitment to chromatin (Homesley *et al*, 2000; Izumi *et al*, 2001; Wohlschlegel *et al*, 2002; Gregan *et al*, 2003; Lee *et al*, 2003; Ricke & Bielinsky, 2004; Sawyer *et al*, 2004). In both yeast and *Xenopus*, Mcm10 loading is required for Cdc45 recruitment to chromatin (Wohlschlegel *et al*, 2002; Gregan *et al*, 2003; Sawyer *et al*, 2004).

In human cells, MCM10 is regulated by proteolysis and phosphorylation in a cell-cycle-dependent manner, with protein levels and chromatin association highest during S phase and displacement from chromatin in G2 phase (Izumi *et al*, 2000, 2004). Similar recruitment to DNA replication origins in a cell-cycle-regulated manner was reported for yeast Mcm10 (Ricke & Bielinsky, 2004).

In yeast, free Mcm10 stabilizes DNA polymerase α-primase through complex formation and targets the polymerase to the origin (Fien *et al*, 2004; Ricke & Bielinsky, 2004, 2006). Moreover, it has been shown that fission yeast Mcm10 can bind to double-stranded (ds) and single-stranded (ss) DNA and contains a primase activity (Fien *et al*, 2004; Fien & Hurwitz, 2006). In addition to forming complexes with DNA polymerase α-primase, budding yeast Mcm10 also interacts with DNA polymerases δ and

[1]Department of Pathology, University College London, London WC1E 6JJ, UK
[2]Wolfson Institute for Biomedical Research, University College London, Cruciform Building, Gower Street, London WC1E 6BT, UK
[3]School of Crystallography, Birkbeck College, Bloomsbury, Malet Street, London WC1E 7HX, UK
[4]Department of Biochemistry & Molecular Biology, 1.224 Medical Research Building, University of Texas Medical Branch, Galveston, Texas 77555-1055, USA
[+]Corresponding author. Tel: +44 20 7679 0959; Fax: +44 20 7388 4408; E-mail: a.okorokov@ucl.ac.uk
[++]Corresponding author. Tel: +44 (0) 20 7631 6845; Fax: +44 (0) 20 7631 6803; E-mail: e.orlova@mail.cryst.bbk.ac.uk

Received 28 March 2007; revised 2 August 2007; accepted 2 August 2007; published online 7 September 2007

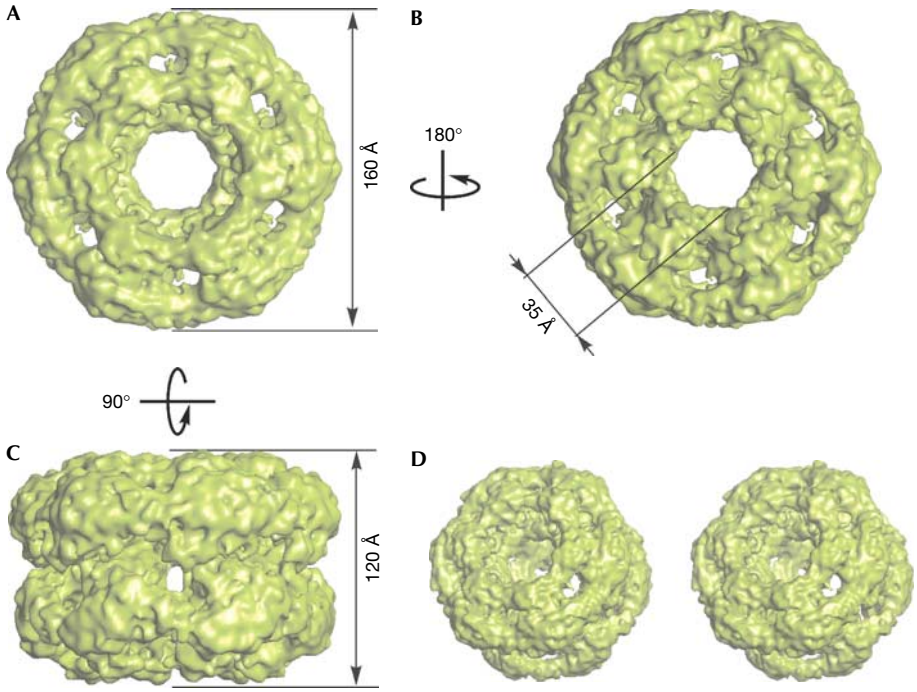

Fig 1 | Surface representation of the MCM10 three-dimensional reconstruction at 16 Å resolution. The ring-shaped MCM10 molecule was viewed at different angles: (**A**) top view, (**B**) bottom view, (**C**) side view and (**D**) stereo view. The surface rendering is shown at 1σ density threshold. MCM10, minichromosome maintenance 10.

ε (Kawasaki *et al*, 2000). Mutations in yeast Mcm10 show defects in the completion of S phase, suggesting that in addition to its function in replication initiation Mcm10 might participate in the elongation phase (Merchant *et al*, 1997; Kawasaki *et al*, 2000).

Human MCM10 is a 98 kDa protein of 874 amino acids, which contains a CCCH-type zinc-finger motif in its central part that seems to be conserved among homologues from yeast to mammals (Izumi *et al*, 2000; Cook *et al*, 2003). MCM10 interacts with numerous replication initiation factors, but it shows low homology across species and lacks marked similarities to other proteins at the sequence level (Hart *et al*, 2002; Christensen & Tye, 2003; Lee *et al*, 2003). The deficiency in conserved protein domains and motifs in the MCM10 sequence has so far obscured understanding its role in the molecular replication machinery. In this study, we used electron microscopy and single-particle analysis to shed some light on the nature of this essential protein and report the first structure, to our knowledge, of full-length human MCM10 protein.

RESULTS AND DISCUSSION

Electron microscopy and 3D reconstruction of MCM10

Recombinant human MCM10 protein was expressed and purified to homogeneity from *Escherichia coli* and analysed by electron microscopy and single-particle analysis (supplementary Figs 1 and 2 online). The three-dimensional map of the protein was obtained at 16 Å resolution at 0.5 threshold of the Fourier shell correlation function. The overall shape of the MCM10 molecule is a double-layered ring assembly with a sixfold symmetry. The height of the molecule is 120 Å and the diameter is 160 Å (Fig 1). The axial channel has a variable diameter (Figs 1,2). The ring is split into two layers (tiers) by six radial channels with entrances of an elliptical shape (10 Å × 20 Å) located in the middle of the ring structure (Figs 1C and 2, sections 4 and 5). The top and bottom tiers are distinct. The top tier has a dense rim (Fig 1A). Six bent lateral channels start outside the top rim and penetrate both tiers. The channels have entrances of approximately 10 Å in diameter and exits of approximately 25 Å × 30 Å at the bottom of the molecule (Fig 1A,B,D). Two rings of density within the top tier are separated by an inner chamber with six interconnected compartments (20 Å × 30 Å × 40 Å; Fig 2, section 3). The inner ring forms part of the axial channel wall and the outer ring with dense nodes forms the outer rim of the top tier. The bottom tier has six clearly visible petal-shaped nodes (Fig 1B). This tier has an inner ring of density that narrows the axial channel (Fig 2, section 7). Unlike the top, the bottom tier does not have a chamber and is formed by six separate densities that protrude from the lower inner ring. The axial channel is approximately 40 Å in diameter at the top, around 60 Å at its widest in the central cavity and at the exit at the bottom (Fig 2, sections 1, 4 and 8), and about 35 Å at its narrowest points within the two inner rings (Fig 2, sections 3 and 6). The two tiers are held together by six connections separated by radial channels (~20 Å in diameter). The top of the molecule has a clockwise handedness, which changes to the opposite direction in the bottom part (Fig 2). The molecular mass of MCM10 from electron microscopic data is consistent with the size observed by size-exclusion chromatography and with the molecular mass of 580 kDa ($s = 19.7$S) obtained by analytical ultracentrifugation (see supplementary information online).

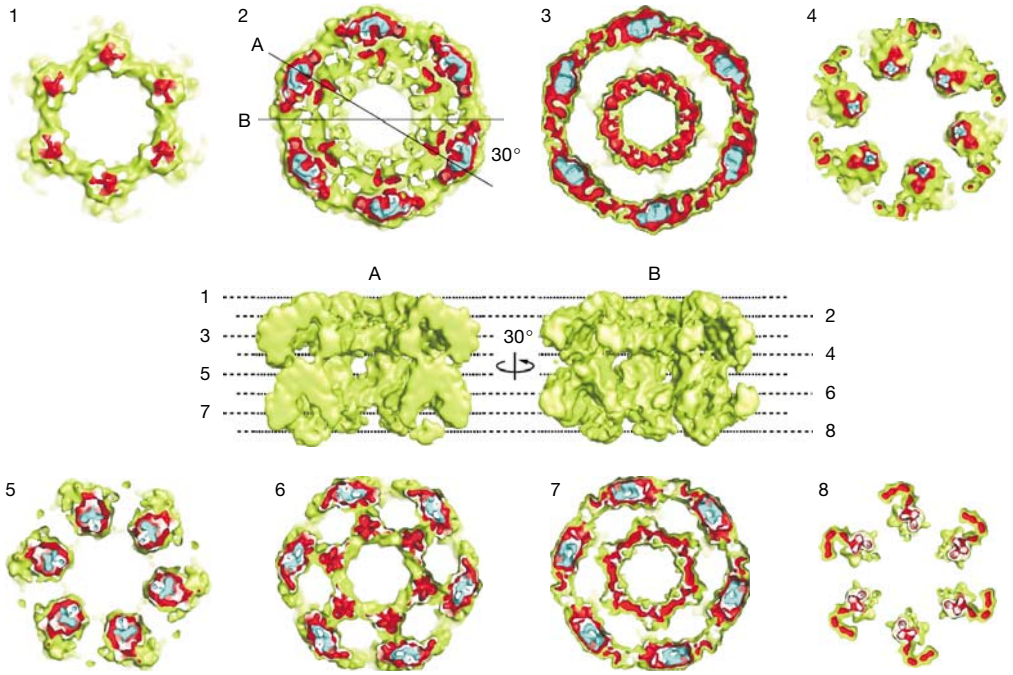

Fig 2 | Inner organization of the MCM10 molecule. Horizontal 16-Å-thick sections of the density map (1–8) and two cut-away views made with a rotation of 30° around the vertical axis (A and B) are shown. Three density levels corresponding to different σ thresholds are shown in green (1σ), red (3σ) and blue (5σ), respectively. The 1σ level depicts the outer shell of the whole molecule, whereas 2σ and 3σ correspond to predominantly α-helical- and β-strand-type formations within the molecule. Dashed lines show planes of the corresponding sections. MCM10, minichromosome maintenance 10.

Model fitting

Despite the lack of homology at sequence level, the global fold of the MCM10 hexamer is reminiscent of several ring-shaped DNA-binding proteins (Hingorani & O'Donnell, 1998). Secondary structure prediction showed two large regions of the MCM10 sequence, which could be identified as independent domains (Fig 3A,B). The first region is formed by approximately 250 amino-acid (aa) residues (220–470), with a predicted secondary structure represented primarily by β-strands. This region contains a conserved CCCH-type zinc-finger motif (Izumi *et al*, 2000; Cook *et al*, 2003). There is a close similarity between the predicted secondary structure for this region of MCM10 and the atomic structure of the amino-terminal domain of the *Methanobacterium thermoautotrophicum* MCM DNA helicase (mtMCM; Fletcher *et al*, 2003), including the positioning of the zinc fingers in both proteins (Fig 3A). The second region of the MCM10 protein (640–874 aa) is predicted to be mainly α-helical (Fig 3B). The region has eight conserved cysteine residues that are clustered in two groups, thus potentially forming at least one additional zinc finger in the 782–835 aa residues region. The secondary structure prediction for the carboxy-terminal part of MCM10 shows close similarity to the architecture of the simian virus 40 (SV40) large T-antigen (SV40 LTag) C-terminal domain (Fig 3B; Li *et al*, 2003).

We therefore used the atomic structures of mtMCM and SV40 LTag (Protein Data Bank entries 1N25 and 1LTL, respectively) for docking into our human MCM10 three-dimensional map. These domains were localized by the automated search with URO software (Navaza *et al*, 2002). The fitting unambiguously positioned the SV40 LTag and mtMCM domains in the top and bottom layer of the MCM10 three-dimensional map, respectively, with a high correlation coefficient of 0.7 for each (Fig 3C).

The orientation of the mtMCM domains within the bottom ring coincides with their orientation in the mtMCM hexameric structure (Fletcher *et al*, 2003). According to the fitting results, the zinc fingers of both domains are likely to be positioned on the outer surface of the molecule (Fig 3). The zinc fingers of the mtMCM domain are putatively located in the petal-shaped nodes at the bottom of the three-dimensional map facing outwards (Fig 2, section 8), whereas the zinc fingers of the SV40 LTag domain are placed in the top rim of the molecule (Fig 2, section 1). Both structures used for docking are smaller than the respective layers of MCM10 density and leave enough room for additional ~100 and ~200 aa residues for the top and bottom parts of the monomer, respectively. However, the main density features within the two-tiered ring are well occupied (Fig 3C–E), indicating a high similarity between the MCM10 architecture and organization of mtMCM and SV40 LTag proteins. The remarkable similarity of the MCM10 inner chambers and channels with known DNA helicase structures indicates that MCM10 might also use this architecture for a ssDNA passage, for example, for the recently discovered primase activity (Fien & Hurwitz, 2006).

DNA-binding properties of MCM10

The ring-shaped structure of MCM10 suggests that this replication protein might have conserved the ability to bind to DNA by circular assembly similarly to other proteins involved in DNA metabolism (Hingorani & O'Donnell, 1998), thus forming a topological link and structural scaffold between replication factors

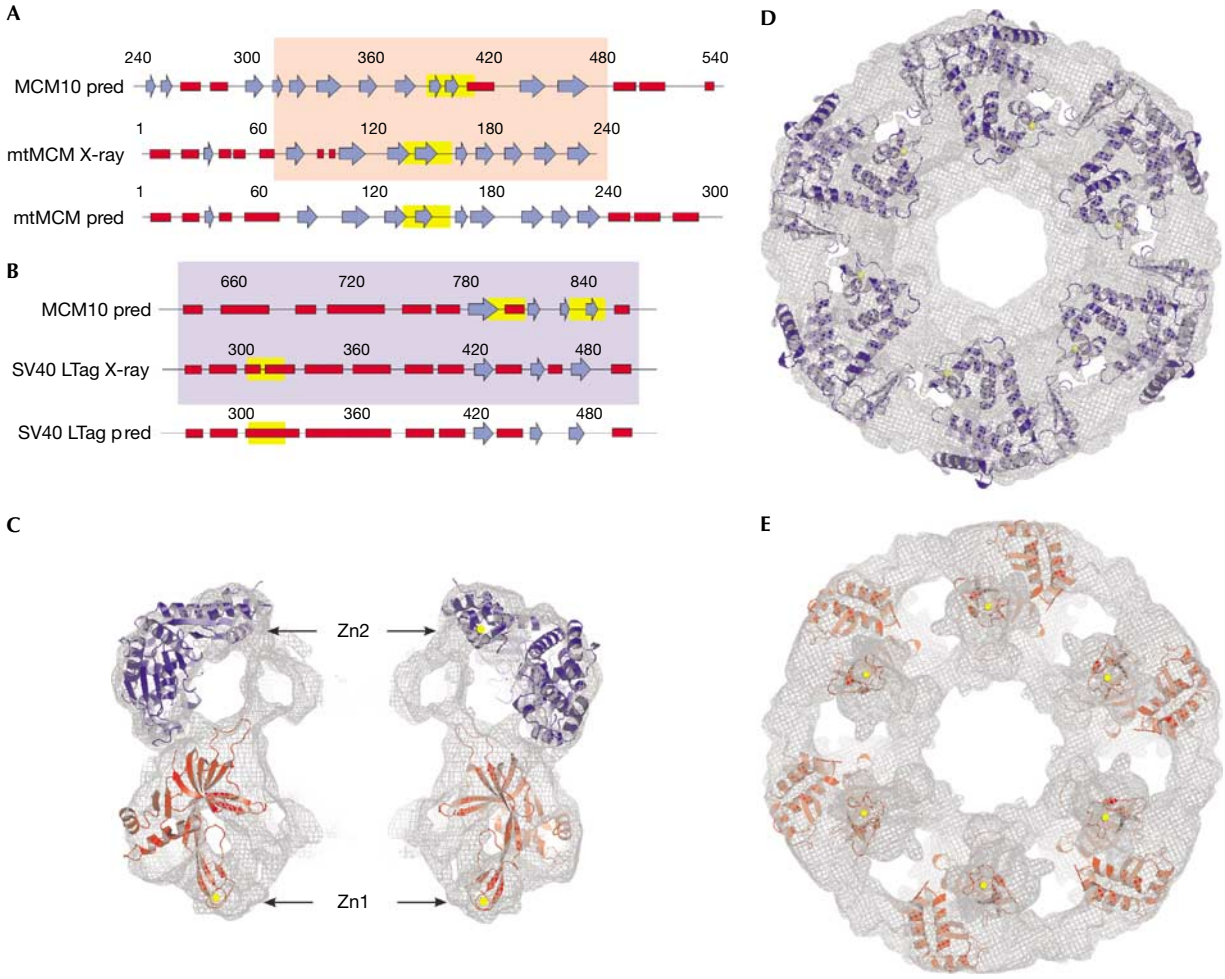

Fig 3 | Secondary structure comparison and model fitting. Comparison of the secondary structure prediction (pred) for the MCM10 molecule with crystal structure and secondary structure prediction of (**A**) mtMCM and (**B**) SV40 LTag. Red rectangular boxes represent α-helices, and blue arrows represent β-strands. The secondary structure assigned to the crystal structures of mtMCM and SV40 LTag correlates well with the predicted structure of MCM10 in the 240–480 and 640–870 amino-acid regions, respectively (highlighted by pink and blue boxes). Zinc-finger-binding clusters are indicated by yellow boxes. (**C**) The central slice of the structure with fitted SV40 LTag and mtMCM domains. Zinc atoms are depicted as yellow spheres and indicated by arrows. (**D**) The top tier of the MCM10 three-dimensional map at threshold 1σ with fitted atomic coordinates of SV40 LTag (in blue). (**E**) mtMCM amino-terminal domain (in red) fitted into the bottom tier of the reconstruction. MCM10, minichromosome maintenance 10; mtMCM, *Methanobacterium thermoautotrophicum* MCM DNA helicase; SV40, simian virus 40; SV40 LTag, large T-antigen.

and the origin. To accomplish this, MCM10 should bind to DNA, which was tested by using wild-type MCM10 and two site-directed mutants (Cys399Tyr and Cys796Ala) designed to destabilize the respective zinc fingers in a DNA-binding assay. The Cys399Tyr mutation has previously been reported to inactivate MCM10 function in yeast (Homesley *et al*, 2000; Cook *et al*, 2003). Recombinant wild-type MCM10 was able to bind efficiently to ssDNA as determined by electromobility shift assay; however, both zinc-finger mutants had impaired ssDNA binding (Fig 4A).

Next, we tested whether MCM10 could bind to dsDNA by using a 250-bp-long blunt-ended DNA fragment with biotinylated ends, thus enabling us to trap MCM10 if it slides off the DNA. Our data show that stable complexes of MCM10 with dsDNA were observed only when the DNA ends were blocked by streptavidin, suggesting a sliding clamp type of binding (Fig 4B). These data were further supported by examining (i) MCM10–DNA complexes treated with restriction enzyme *Bam*HI and (ii) dsDNA targets for which only one DNA end could be blocked by streptavidin. No complexes of MCM10 with dsDNA were observed in either case (see supplementary information online). Notably, zinc-finger mutants of MCM10 did not form complexes with dsDNA with or without DNA-end block (data not shown), confirming that the zinc fingers of MCM10 are important in DNA binding and/or stability of the protein–DNA complex.

Biological implications

The ring-shaped 'helicase-like' structural organization of human MCM10 suggests two models for its molecular evolution. In one model, MCM10 evolved similarly to many other ring-shaped

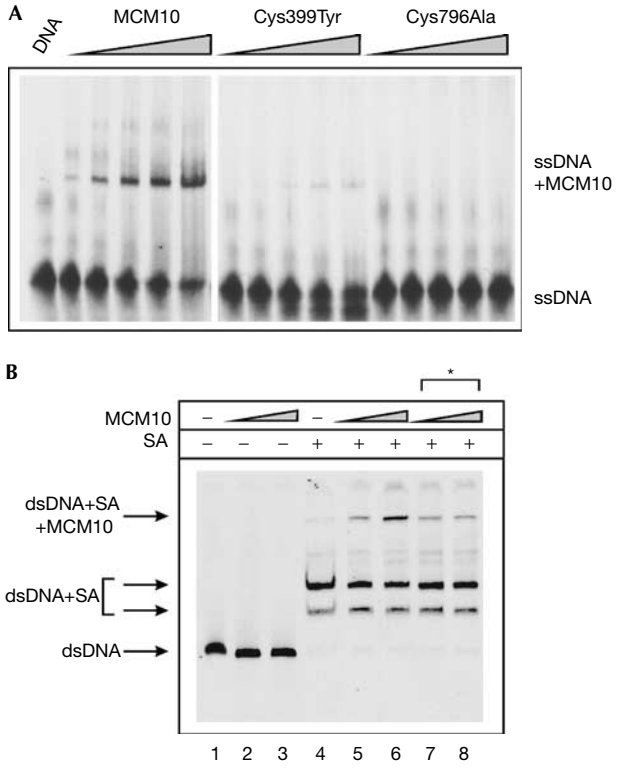

Fig 4 | DNA-binding properties of MCM10. (**A**) Increasing amounts of purified MCM10 wild-type, Cys399Tyr and Cys796Ala proteins (25, 50, 75, 100 and 150 ng) were incubated with radiolabelled ssDNA and analysed by gel-shift assay. The MCM10–ssDNA slow migrating complexes were visible only when wild-type MCM10 was present. (**B**) Increasing amounts of MCM10 (50 and 100 ng) were incubated with 5′-biotinylated radiolabelled dsDNA in the absence (lanes 2 and 3) or presence (lanes 5–8) of streptavidin (SA). Lanes 5 and 6: MCM10 and streptavidin were added to DNA at the same time; lanes 7 and 8: DNA was preincubated with streptavidin for 10 min (indicated by asterisk). DNA alone and in the presence of streptavidin is shown in lanes 1 and 4, respectively. dsDNA, double-stranded DNA; MCM10, minichromosome maintenance 10; ssDNA, single-stranded DNA.

oligomeric DNA-binding proteins by using their architecture to provide the most processive topological link with DNA (Hingorani & O'Donnell, 1998). The second model follows an evolutionary path from a hexameric DNA helicase ancestor, from which MCM10 inherited the fold. As a renegade protein, MCM10 then lost its helicase activity for a structural supportive role as a 'docking' module aimed to facilitate protein–protein interactions between DNA replication proteins. Consistent with this latter hypothesis, the MCM10 molecule shows remarkable structural similarity to DNA helicases (Patel & Picha, 2000; Pape *et al*, 2003; Chen *et al*, 2005), but has no conserved helicase motifs within its sequence and no detectable DNA helicase activity *in vitro* (data not shown). Both models would result in the ring shape, providing a structural basis for MCM10 interaction with essential replication factors simultaneously, perhaps linking the Mcm2–7 helicase ring on one side and DNA Pol-α primase on the other.

Taken together, the ability of MCM10 to bind to DNA in a sliding clamp manner, and the location of zinc fingers, as predicted by model fitting (Figs 3,4), suggest a possible molecular mechanism by which MCM10 facilitates protein–protein interactions during the pre-RC to pre-IC transition and later during the elongation stage. The putative arrangement of DNA within the MCM10 ring would provide for processivity and free movement on DNA, and thus could explain the reported MCM10 requirement for fork progression by maintaining contact between the replicative helicase and polymerases (Ricke & Bielinsky, 2004; Pacek *et al*, 2006).

In conclusion, here we have reported the first, to our knowledge, molecular structure of the DNA replication factor MCM10. Our model is supported by biochemical data and shows that MCM10 assembles into a hexameric ring. This organization allows stable association with DNA and potentially facilitates protein–protein interactions within the DNA-replication machinery, explaining the MCM10 requirement for replication initiation and elongation.

METHODS

Recombinant human MCM10. Human MCM10 complementary DNA was cloned into pET100/D-TOPO vector (Invitrogen, Paisley, UK) and expressed in *E. coli* strain Rosetta (Novagen, Nottingham, UK) (see supplementary information online). MCM10 protein was purified by Ni^{2+} affinity chromatography, followed by removal of the His tag with tobacco etch virus (TEV) protease and further gel filtration on Superose 6 column in 25 mM Tris–HCl (pH 7.5), 150 mM NaCl, 10 mM $MgCl_2$ and 25 mM KCl. The purity and identity of the protein sample used for electron microscopic analysis was verified by mass spectrometry and protein sequencing.

Electron microscopy, image processing and model fitting. MCM10 protein samples (0.01 mg/ml) were stained with 2% w/v methylamine tungstate, pH 6.8 (Nano-W, Nanoprobes Inc., Yaphank, NY, USA). Micrographs were recorded on a Kodak SO163 film using an FEI Tecnai T10 microscope in low-dose mode, operated at an accelerating voltage of 100 kV, with a magnification of ×44,000. Micrographs were digitized with a step size of 7 μm corresponding to a pixel size of 1.59 Å. Particle images of MCM10 (~5,000) were selected manually and analysed using IMAGIC-5 (van Heel *et al*, 1996; supplementary information online). Secondary structure prediction was carried out using the PredictProtein server (EMBL, Heidelberg, Germany, http://www.embl-heidelberg.de/predictprotein/predictprotein.html). Domain fitting into the three-dimensional map of MCM10 was carried out automatically using URO (Navaza *et al*, 2002). The electron microscopic map of human MCM10 protein has been deposited in the macromolecular structure database (EBI) with accession number EMD-1254.

DNA-binding and DNA helicase activity assays. DNA-binding properties of MCM10 and its mutants were studied by electromobility shift assay (supplementary information online). The final volume of reactions was 20 μl in 10 mM Tris–HCl (pH 8.0), 150 mM NaCl, 5 mM $MgCl_2$ and 2 mM dithiothreitol buffer. Samples were analysed using 6% 0.5× TBE Novex DNA Retardation gels (Invitrogen) at 120 V, 4 °C. Gels were then dried and analysed by autoradiography.

Supplementary information is available at *EMBO reports* online (http://www.emboreports.org).

ACKNOWLEDGEMENTS

We are grateful to H. Saibil for stimulating discussions, R. Westlake and D. Houldershaw for computational support, L. Wang for assistance in microscopy and R. Sarra for help with analytical ultracentrifugation. This work has been funded by Cancer Research UK Programme Grant C428/A6263 to G.H.W., K.S. and A.L.O., and University College of London Charities and the Royal Free and University College Medical School Project Grant F124 to A.L.O.

REFERENCES

Bell SP, Dutta A (2002) DNA replication in eukaryotic cells. *Annu Rev Biochem* **71:** 333–374

Chen YJ, Yu X, Kasiviswanathan R, Shin JH, Kelman Z, Egelman EH (2005) Structural polymorphism of *Methanothermobacter thermautotrophicus* MCM. *J Mol Biol* **346:** 389–394

Christensen TW, Tye BK (2003) *Drosophila* MCM10 interacts with members of the prereplication complex and is required for proper chromosome condensation. *Mol Biol Cell* **14:** 2206–2215

Cook CR, Kung G, Peterson FC, Volkman BF, Lei M (2003) A novel zinc finger is required for Mcm10 homocomplex assembly. *J Biol Chem* **278:** 36051–36058

Fien K, Hurwitz J (2006) Fission yeast Mcm10p contains primase activity. *J Biol Chem* **281:** 22248–22260

Fien K, Cho YS, Lee JK, Raychaudhuri S, Tappin I, Hurwitz J (2004) Primer utilization by DNA polymerase α-primase is influenced by its interaction with Mcm10p. *J Biol Chem* **279:** 16144–16153

Fletcher RJ, Bishop BE, Leon RP, Sclafani RA, Ogata CM, Chen XS (2003) The structure and function of MCM from archaeal *M. thermoautotrophicum*. *Nat Struct Biol* **10:** 160–167

Gregan J, Lindner K, Brimage L, Franklin R, Namdar M, Hart EA, Aves SJ, Kearsey SE (2003) Fission yeast Cdc23/Mcm10 functions after pre-replicative complex formation to promote Cdc45 chromatin binding. *Mol Biol Cell* **14:** 3876–3887

Hart EA, Bryant JA, Moore K, Aves SJ (2002) Fission yeast Cdc23 interactions with DNA replication initiation proteins. *Curr Genet* **41:** 342–348

Hingorani MM, O'Donnell M (1998) Toroidal proteins: running rings around DNA. *Curr Biol* **8:** R83–R86

Homesley L, Lei M, Kawasaki Y, Sawyer S, Christensen T, Tye BK (2000) Mcm10 and the MCM2–7 complex interact to initiate DNA synthesis and to release replication factors from origins. *Genes Dev* **14:** 913–926

Izumi M, Yanagi K, Mizuno T, Yokoi M, Kawasaki Y, Moon KY, Hurwitz J, Yatagai F, Hanaoka F (2000) The human homolog of *Saccharomyces cerevisiae* Mcm10 interacts with replication factors and dissociates from nuclease-resistant nuclear structures in G(2) phase. *Nucleic Acids Res* **28:** 4769–4777

Izumi M, Yatagai F, Hanaoka F (2001) Cell cycle-dependent proteolysis and phosphorylation of human Mcm10. *J Biol Chem* **276:** 48526–48531

Izumi M, Yatagai F, Hanaoka F (2004) Localization of human Mcm10 is spatially and temporally regulated during the S phase. *J Biol Chem* **279:** 32569–32577

Kawasaki Y, Hiraga S, Sugino A (2000) Interactions between Mcm10p and other replication factors are required for proper initiation and elongation of chromosomal DNA replication in *Saccharomyces cerevisiae*. *Genes Cells* **5:** 975–989

Lee JK, Seo YS, Hurwitz J (2003) The Cdc23 (Mcm10) protein is required for the phosphorylation of minichromosome maintenance complex by the Dfp1-Hsk1 kinase. *Proc Natl Acad Sci USA* **100:** 2334–2339

Li D, Zhao R, Lilyestrom W, Gai D, Zhang R, DeCaprio JA, Fanning E, Jochimiak A, Szakonyi G, Chen XS (2003) Structure of the replicative helicase of the oncoprotein SV40 large tumour antigen. *Nature* **423:** 512–518

Maine GT, Sinha P, Tye BK (1984) Mutants of *S. cerevisiae* defective in the maintenance of minichromosomes. *Genetics* **106:** 365–385

Maiorano D, Lutzmann M, Mechali M (2006) MCM proteins and DNA replication. *Curr Opin Cell Biol* **18:** 130–136

Mendez J, Stillman B (2003) Perpetuating the double helix: molecular machines at eukaryotic DNA replication origins. *BioEssays* **25:** 1158–1167

Merchant AM, Kawasaki Y, Chen Y, Lei M, Tye BK (1997) A lesion in the DNA replication initiation factor Mcm10 induces pausing of elongation forks through chromosomal replication origins in *Saccharomyces cerevisiae*. *Mol Cell Biol* **17:** 3261–3271

Navaza J, Lepault J, Rey FA, Alvarez-Rua C, Borge J (2002) On the fitting of model electron densities into EM reconstructions: a reciprocal-space formulation. *Acta Crystallogr D* **58:** 1820–1825

Pacek M, Tutter AV, Kubota Y, Takisawa H, Walter JC (2006) Localization of MCM2–7, Cdc45, and GINS to the site of DNA unwinding during eukaryotic DNA replication. *Mol Cell* **21:** 581–587

Pape T, Meka H, Chen S, Vicentini G, van Heel M, Onesti S (2003) Hexameric ring structure of the full-length archaeal MCM protein complex. *EMBO Rep* **4:** 1079–1083

Patel SS, Picha KM (2000) Structure and function of hexameric helicases. *Annu Rev Biochem* **69:** 651–697

Ricke RM, Bielinsky AK (2004) Mcm10 regulates the stability and chromatin association of DNA polymerase-α. *Mol Cell* **16:** 173–185

Ricke RM, Bielinsky AK (2006) A conserved Hsp10-like domain in Mcm10 is required to stabilize the catalytic subunit of DNA polymerase-α in budding yeast. *J Biol Chem* **281:** 18414–18425

Sawyer SL, Cheng IH, Chai W, Tye BK (2004) Mcm10 and Cdc45 cooperate in origin activation in *Saccharomyces cerevisiae*. *J Mol Biol* **340:** 195–202

Takeda DY, Dutta A (2005) DNA replication and progression through S phase. *Oncogene* **24:** 2827–2843

van Heel M, Harauz G, Orlova EV, Schmidt R, Schatz M (1996) A new generation of the IMAGIC image processing system. *J Struct Biol* **116:** 17–24

Wohlschlegel JA, Dhar SK, Prokhorova TA, Dutta A, Walter JC (2002) *Xenopus* Mcm10 binds to origins of DNA replication after Mcm2–7 and stimulates origin binding of Cdc45. *Mol Cell* **9:** 233–240